

CURRENT STATUS OF CTI TARGET SYSTEMS FOR THE PRODUCTION OF PET RADIOCHEMICALS

B.W. Wieland, G.T. Bida, H.C. Padgett and G.O. Hendry
CTI Cyclotron Systems, Berkeley, California USA

INTRODUCTION

Research on targets for an 11 MeV negative-ion cyclotron was initiated in July 1985, and proof-of-principle prototypes were reported¹⁻⁴ in June 1986. Continuing development has resulted in commercially available target systems for producing PET radiochemicals. Five hospital PET centers now use two to four targets routinely.⁵ Two of these sites⁶ utilize a cost-effective, technician-operated, integrated Radionuclide Delivery System⁷ consisting of: surface-shielded 11 MeV negative-ion proton cyclotron, target systems, radiochemical synthesis modules,⁸ and menu-driven computer control capability. Two additional hospital units of this type are in the start-up phase.⁹ Three more are under construction¹⁰ for 1989 installation. Six additional systems are in the planning stage for 1990 installation.¹¹

This paper includes: target experience resulting from routine hospital use, testing at our laboratories to further characterize standard targets, and work-in-progress on systems to be made available in the future.

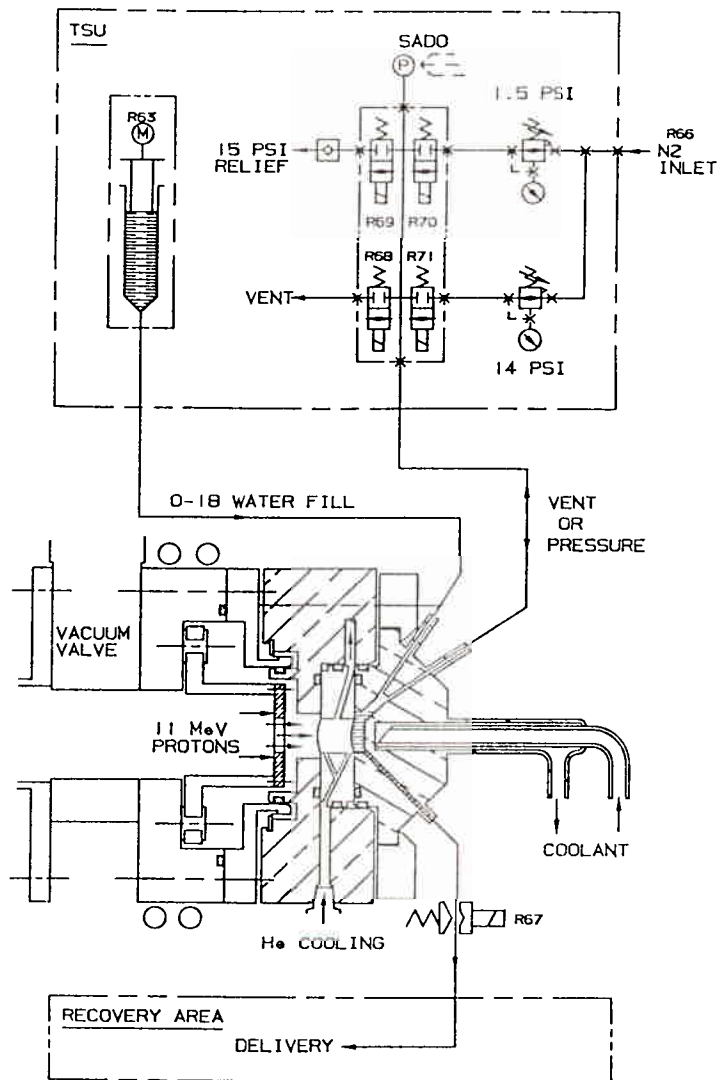
[¹⁸O]Water/[¹⁸F]Fluoride Ion Targets

Key features of the water target are as follows:

- 1) Small economical target loading of 0.33 mL [¹⁸O]water minimizes evaporation steps in chemical synthesis and eliminates the need to recycle enriched water;
- 2) Reflux space (0.30 mL) provides good heat transfer allowing efficient 20 μ A bombardments;
- 3) Low radiolysis losses with uniform reproducible beam optics and selectable collimator transmission (available from RDS 11 MeV negative-ion cyclotron);
- 4) Menu-driven computer control of target loading and recovery (at distances up to 30 meters);
- 5) Routine hospital yields of about 500 mCi in one hour for nickel plated copper target with Havar window;
- 6) Optional unplated design can be constructed with same or different material for body, window, and solderless fittings (see laboratory data for silver body and window).

Figure 1 indicates the components of the [¹⁸F]fluoride ion system, which includes both the target and the target support unit (TSU). Production of fluoride ion using the nickel-plated copper target² shown in the schematic is being carried out at five hospital PET centers.⁵ A typical run is 500 mCi from a one hour bombardment. By early 1989, these sites had synthesized over 700 batches of [¹⁸F]FDG and completed more than 1500 patient studies using the CTI Chemistry Process Control Unit (CPCU). This is a general purpose microprocessor-controlled chemical synthesis device⁸ which can be user programmed to carry out a variety of organic and inorganic chemical processes remotely and automatically using an IBM PC/AT or equivalent computer. There are eight CPCU's in operation and seven more scheduled for installation.

As a response to customer requests, we have designed and started characterization experiments on a solid silver target with a silver window. The basic design offers the flexibility of constructing a minimum size target chamber of any unplated or plated metal. Also, since it utilizes solderless entry and exit hardware, any metal can be used for these tubes, and any window material can be chosen. Nine runs have been made to begin the characterization of this target, which has the same internal geometry as the nickel-plated copper target in current hospital use. Results are presented in Table I and discussed below for a target with a 99.99% silver body, 0.001-inch silver window, and stainless steel entry and exit tubes.



A1221057 REV. A

FIGURE 1. ^{18}F FLUORIDE ION PRODUCTION

Table I. Silver Target Performance Data

| μA | Min. | Transmission % | mCi EOB | rinse % | cc gas | mCi/ μA |
|---------|------|----------------|---------|---------|--------|--------------|
| 10 | 10 | 59 | 86 | 6 | --- | 140 |
| 20 | 10 | 58 | 139 | 5 | --- | 114 |
| 20 | 10 | 87 | 145 | 4 | --- | 118 |
| 20 | 120 | 58 | 1036 | 6 | 86 | 98 |
| 20 | 120 | 82 | 1092 | 11 | 108 | 103 |
| 20 | 120 | 56 | 1034 | 5 | 110 | 95 |
| 20 | 120 | 54 | 1060 | 9 | 67 | 101 |
| 20 | 120 | 82 | 1022 | 11 | 90 | 96 |
| 20 | 120 | 82 | 1168 | 5 | 95 | 111 |

Collimator transmission percent was varied by using two different extraction foil thickness (approximately 1 and 25 micron). The rinse was used to assess activity loss due to droplets remaining in the target and recovery transfer line, and to obtain the total mCi EOB shown (in order to calculate saturation yield). In a routine hospital run, the activity available for synthesis would be the mCi EOB less the rinse percent, and less an approximate four minute decay from the gentle recovery process used to deliver the 0.33 mL target load. The radiolysis gas evolution of about 100 cc represents a target water loss of 55 μL (16%) for two-hour runs. Some of the variation in yields is due to experimenting with target water loading and recovery techniques.

The silver window used in these tests reduces the energy on target water from 10.7 MeV (for the previously used thin Havar window) to 10.4 MeV. The yields, however, are slightly better, which may be due to the higher thermal conductivities of the body (Ag vs Cu) and especially the window (Ag vs Havar). There may be other effects, such as the different metal ion environment.

This target has been used at UCLA by N. Satyamurthy to produce [^{18}F]fluoride ion and synthesize [^{18}F]FDG. The recovered target water was used directly in the first reaction without using an intermediate resin column to trap the fluoride ion. Initial results are excellent and careful evaluation of extensive use is in progress. The target now in use at UCLA was shipped without disassembly after being used in our Berkeley laboratories to generate the data presented in the table above.

[^{18}O]Oxygen/[^{18}F]Fluorine Target

Production of [^{18}F]F₂ from the $^{18}O(p,n)^{18}F$ nuclear reaction has been previously reported.¹²⁻¹⁵ However, two of the reported methods¹³⁻¹⁵ involve a two-step irradiation process. A modest departure in approach from our earlier report¹² involving a one-step proton irradiation has provided excellent results. These changes included: 1) a longer target with non-zero volume outside the beam strike, employing a water-cooled single-port gold-plated copper body with a conical bore (beam strike volume = 12.4 cc); 2) irradiations conducted at 10.4 MeV on target; and 3) target gas mixtures including the use of helium/fluorine along with ^{18}O -enriched oxygen. Additional details concerning materials and methods are given elsewhere.¹² It is noted here that no aggressive "passivation" protocol was used to precondition the target. Results of several experiments that involved changes in dose, dose rate and carrier fluorine concentration are shown in Table II (see next page).

Table II. ^{18}F Production with 10.4 MeV Protons on $[^{18}\text{O}]\text{O}_2(+\text{F}_2)$
(Target pressure ranged from 200-300 psia)

| μA | <u>T(irr) in min</u> | <u>Fluorine conc.</u> ($\mu\text{mole/charge}$) | <u>Total ^{18}F</u> <u>at EOB(mCi)</u> | <u>Prod. dist.%</u> | | <u>mCi/μA@</u> <u>Saturation</u> |
|---------------|----------------------|--|---|---------------------|----------------|---|
| | | | | <u>Fluorine</u> | <u>Inserts</u> | |
| 10 | 10 | 16 | 41 | 97 | 3 | 67 |
| 35 | 30 | 16 | 393 | 79 | 21 | 65.2 |
| 10(a) | 10 | 21 | 96 | 92 | 9 | 157 |
| 20 | 10 | 21 | 204 | 90 | 10 | 167 |
| 30 | 10 | 19 | 269 | 90 | 10 | 147 |
| 40 | 10 | 20 | 397 | 88 | 12 | 163 |
| 30 | 60 | 21 | 988 | 87 | 13 | 105 |
| 30(a) | 15 | 20 | 235 | 83 | 17 | 86.9 |
| 30 | 30 | 18 | 511 | 88 | 12 | 98.6 |
| 30 | 45 | 19 | 759 | 87 | 13 | 102 |
| 30 | 60 | 19 | 1006 | 87 | 13 | 107 |
| 10 | 10 | 55 | 102 | 93 | 7 | 167 |
| 30(a) | 15 | 40 | 269 | 81 | 19 | 99.4 |
| 30 | 30 | 53 | 573 | 91 | 9 | 111 |
| 30(a) | 30 | 60 | 467 | 91 | 9 | 90.4 |
| 32.5 | 30 | 68 | 734 | 92 | 8 | 131 |
| 40 | 30 | 60 | 740 | 92 | 8 | 107 |
| 40(a) | 60 | 65 | 929 | 90 | 10 | 73.8 |
| 40 | 60 | 78 | 1103 | 90 | 10 | 87.6 |

(a) Denotes first run of the day wherein no pre-irradiation was conducted.

Notable observations from the data include:

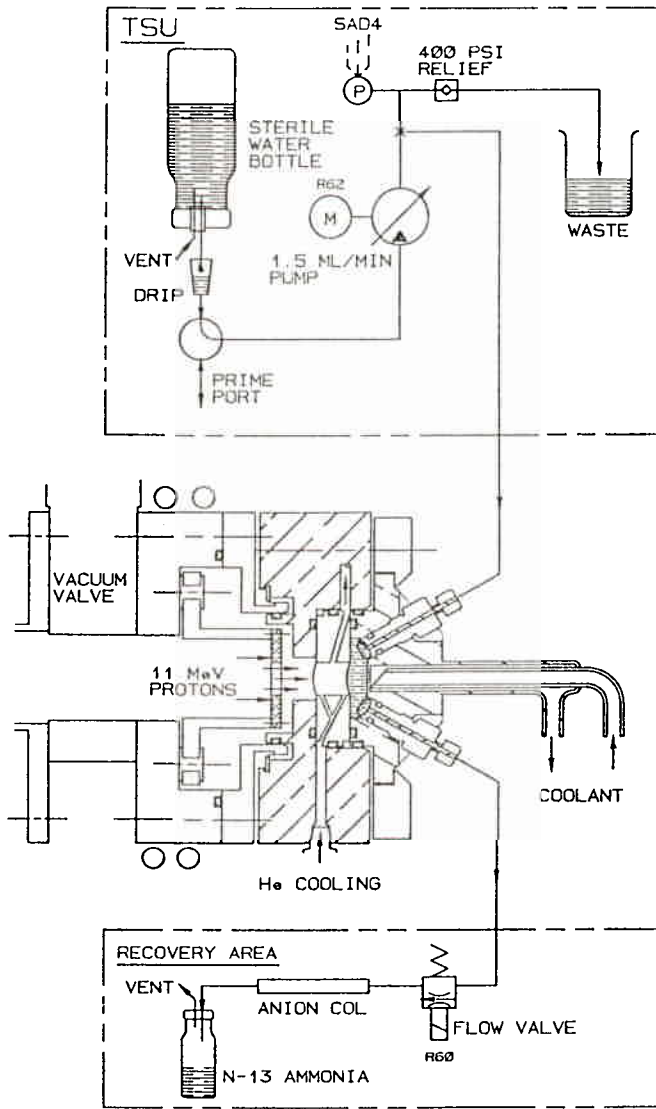
- 1) High activity recovery from the target even at fluorine concentrations as low as 20 μmole per target charge;
- 2) Low inert gas fraction observed under all irradiation conditions investigated
- 3) Insensitivity of target behavior to target gas composition - the second set of eight data listed in the table were generated with a gas mixture that contained as much as 25% helium. All others used a mixture that contained only fluorine and oxygen
- 4) Production of curie quantities of $[^{18}\text{F}]\text{F}_2$ is possible with this target system.

$[^{13}\text{C}]\text{CARBON}/[^{16}\text{O}]\text{WATER SLURRY TARGET FOR PRODUCTION OF } [^{13}\text{N}]\text{AMMONIA}$

The following are some important features of the carbon powder target:

- 1) Economical 0.1 gram loading of amorphous $[^{13}\text{C}]$ powder in natural water;
- 2) In-target chemistry produces $[^{13}\text{N}]\text{ammonia}$ directly in 5 mL batches with no need for subsequent synthesis;
- 3) Product is delivered at 1.5 mL per minute through narrow-bore tube, or alternately transferred (30 meters in 30 seconds) with 30 psi gas pressure;
- 4) Production of over 80 batches (3 μA for 13.5 minutes) before reloading or adding $[^{13}\text{C}]\text{carbon}$ when used for 20 mCi routine hospital doses;
- 5) 150 mCi batches for synthesis applications available with more frequent target loading.

Figure 2 indicates the components of the target system. Production of ammonia using the powder/water slurry target⁴ is being carried out at four hospital PET centers.⁵ Duke University uses a CS-30 cyclotron with the proton beam degraded to 16 MeV on target, while the other three use the RDS11 MeV cyclotron. The targets are identical. The RDS procedure for a 20 mCi patient batch uses a 3 μ A for 13.5 minute run with direct recovery, while the Duke procedure uses a 3 μ A for 7.7 minute run with a 70 foot bolus transfer following EOB using 30 psi nitrogen. Duke University produced about 100 batches in 1989 and the University of Tennessee produced about 200. The targets produce at least 80 batches without addition or reloading of the target.



A122105B REV. A

FIGURE 2. [¹³N]AMMONIUM ION PRODUCTION

Although an amorphous slurry target has produced up to 300 mCi using a 20 μ A for 20 minute run, the results are variable at this level (200-300 mCi), and the target sometimes has to be reloaded immediately. A much more stable operating condition is a 15 μ A beam for 20 minutes with flow cycling, producing about ^{15}O mCi in a 5 ml volume with 4-6 runs between target maintenance.

Although the ^{13}N recoil ion escape fraction for amorphous powder is favorable (about 50%), the beam strike volume is only about 15% carbon (85% water). The powder appears in SEM's to be composed of long fine "hairs" of sub-micron diameter, which apparently do not pack favorably. To overcome this limitation, we are studying several alternate high density forms of carbon slurry utilizing pyrolyzed polymer beads (work in progress by G. Kabalka of University of Tennessee), fluidized bed vapor deposition of [^{13}C]methane on sub-micron seed diamond particles, and use of stacked micron-level evaporated porous carbon films. Loss of ^{13}C starting materials is a major consideration in these approaches. We hope to have at least one type of high-density slurry ready for beam testing by the end of 1989.

GAS TARGETS FOR THE PRODUCTION OF [^{15}O]OXYGEN AND [^{11}C]CARBON DIOXIDE

The gas targets include the following features:

- 1) Custom-designed zero dead volume valves mounted directly on the target body;
- 2) Zero dead volume pressure transducer;
- 3) Valve seats designed for rapid bolus activity delivery or for "metered" activity delivery for steady-state inhalation studies;
- 4) Valve bodies that allow dispensing the activity into a constant flow helium sweep stream;
- 5) Small, zero dead volume (12 cc) beam strike;
- 6) Conical beam strike volume to accommodate small angle multiple scattering of the proton beam.

Figure 3 outlines the features of the gas target for the production of [^{15}O]oxygen as well as the accompanying Target Support Unit (TSU).

Listed in the tables below are typical ^{15}O yields for the various radiolabeled products after processing with the GPU, and the radio-chemical purities found for these products.

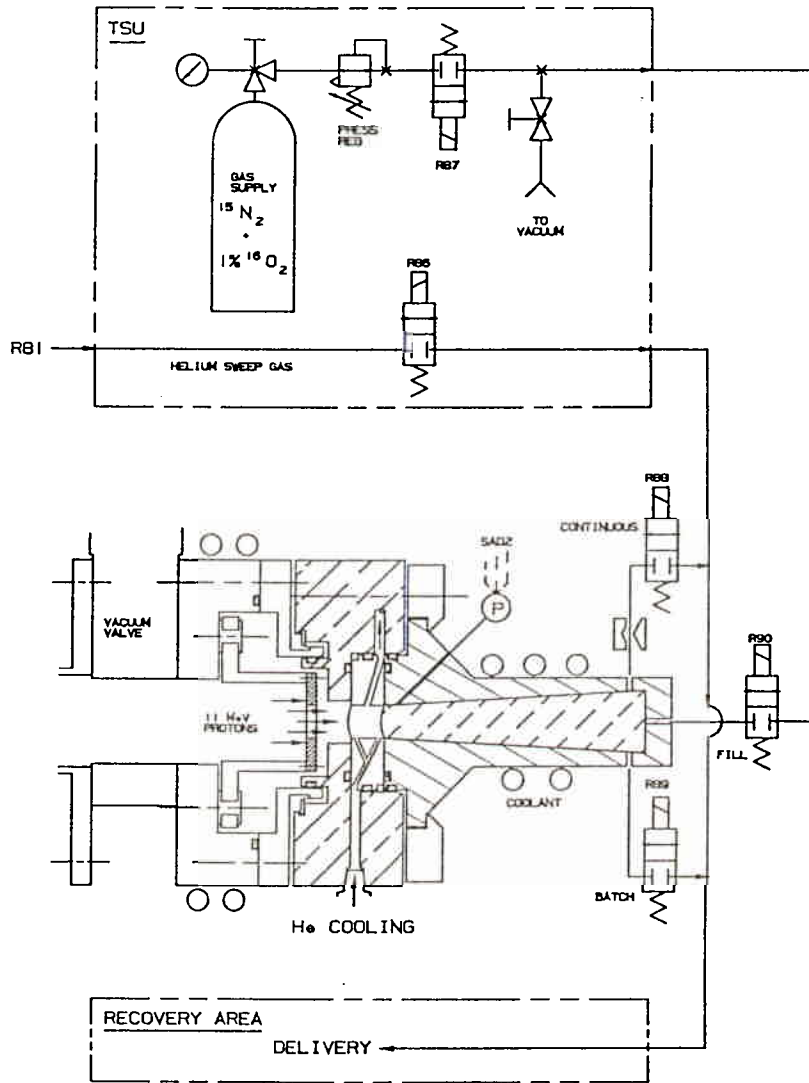


FIGURE 3. [^{15}O] OXYGEN PRODUCTION

A122:059 REV. A

In Table III, the average saturation yield reported for seven runs is 82.3 mCi/ μ A. This value has been determined to be statistically greater than the currently accepted yield²⁰ of 64 mCi/ μ A at our on target energy of 10.4 MeV. Recent results from our laboratory for the production of both ^{11}C and ^{15}O suggest that the yields are strongly dependent upon small angle multiple scattering. In addition, our results for $[^{15}\text{O}]\text{O}_2$ production indicate that a more comprehensive analysis of the cross sections and thick target yields for the $^{15}\text{N}(p,n)^{15}\text{O}$ nuclear reaction is in order.

Table III. Production of $[^{15}\text{O}]$ -labeled compounds at $E_p = 10.4$ MeV
(Target = 200 psia of $[^{15}\text{N}]\text{N}_2$, $40 \mu\text{A} \times 10$ min irradiations).

| Fraction of $[^{15}\text{O}]$ used | $[^{15}\text{O}]$ Product | mCi at end of conversion(a) | Conversion efficiency(b) | mCi/ μA @sat |
|------------------------------------|---------------------------|-----------------------------|--------------------------|-------------------------|
| 0.2 | O_2 | 307 | -- | -- |
| 0.2 | CO | 134 | 48% | -- |
| 0.2 | CO_2 | 143 | 53% | -- |
| 0.2 | H_2O | 247 | 84% | -- |
| 0.9 | O_2 | 1440 | -- | 82.3(c) |
| 0.9 | CO | 1377 | 81% | -- |
| 0.9 | CO_2 | 1340 | 79% | -- |
| 0.9 | H_2O | 1029 | 71% | -- |

(a) Average of five runs for each $[^{15}\text{O}]$ product for the 20% usage experiments.

(b) Calculated based on $[^{15}\text{O}]\text{O}_2$ contained in an equivalent amount of gas dispensed from the target.

(c) Average of seven runs.

Table IV Radio-GC data
Contaminant

| Product | $[^{15}\text{O}]\text{CO}$ | $[^{15}\text{O}]\text{CO}_2$ | $[^{15}\text{O}]\text{O}_2$ | $[^{13}\text{N}]\text{N}_2$ |
|------------------------------|----------------------------|------------------------------|-----------------------------|-----------------------------|
| $[^{15}\text{O}]\text{CO}$ | > 99% | none det. | none det. | < 0.1% |
| $[^{15}\text{O}]\text{CO}_2$ | none det. | > 98% | 1-1.5% | < 0.1% |
| $[^{15}\text{O}]\text{O}_2$ | none det. | none det. | > 99% | < 0.1% |

Figure 4 outlines the features of the gas target for the production of $[^{11}\text{C}]$ carbon dioxide, as well as the accompanying target support unit (TSU). Results for the performance of this target over a range of operating parameters are listed in Table V. Significant improvements in beam optics, alignment and target geometry have resulted in near theoretical yields for ^{11}C production. Thus, the average saturation yield for these nine measurements is about 94% of the value predicted at this energy.¹⁷

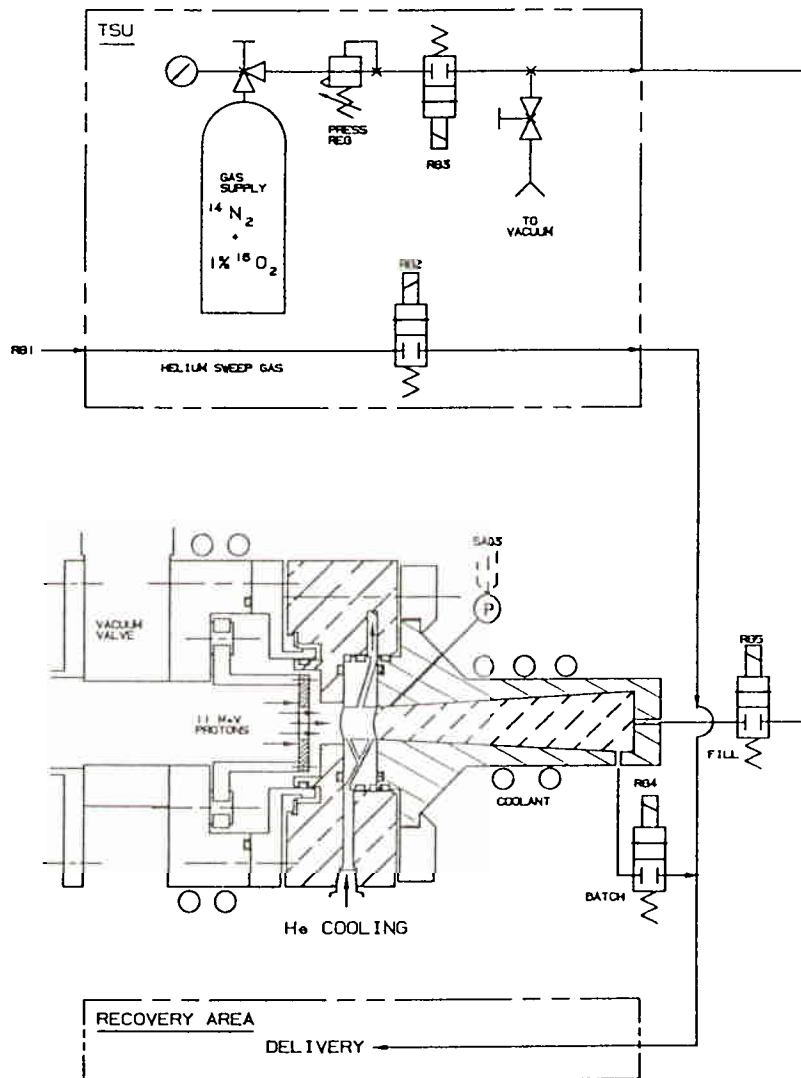


FIGURE 4. ^{11}C CARBON DIOXIDE PRODUCTION

A1221060 REV. A

Table V $[^{11}\text{C}]\text{CO}_2$ Production with 10.4 MeV protons

| μA | <u>T(irr) in min</u> | <u>Psia (no beam)</u> | <u>EOB mCi</u> | <u>mCi/μA@sat</u> |
|---------------|----------------------|-----------------------|----------------|---|
| 20 | 10 | 215 | 379 | 65.8 |
| 30 | 10 | 212 | 596 | 69.0 |
| 40 | 10 | 211 | 802 | 69.6 |
| 20 | 20 | 210 | 655 | 66.4 |
| 30 | 20 | 210 | 992 | 67.1 |
| 40 | 20 | 210 | 1345 | 68.2 |
| 20 | 40 | 212 | 987 | 66.4 |
| 30 | 40 | 210 | 1500 | 67.3 |
| 40 | 40 | 210 | 2091 | 70.4 |

We have measured the specific activity of the $[^{11}\text{C}]\text{CO}_2$ produced with the CTI Carbon-11 gas target using radio-GC. The data are summarized in Table VI. Several factors can affect the specific activity of the carbon dioxide, some of which have been discussed in^{16,18}. The relatively high specific activities reported here for $[^{11}\text{C}]\text{CO}_2$ may reflect lower amounts of carrier carbon present because of the small target charge of $[^{14}\text{N}]\text{N}_2$ and/or the minimal beam strike surface area of the target body.

Table VI. Specific activity data for production of $[^{11}\text{C}]\text{CO}_2$ at $E_p = 10.4$ MeV

| μA | <u>T(irr) in min</u> | <u>mCi of $[^{11}\text{C}]\text{CO}_2$ sampled</u> | <u>μmol of $[^{12}\text{C}]\text{CO}_2$</u> | <u>Sp. Act. in $\text{Ci}/\mu\text{mol}$</u> |
|---------------|----------------------|---|--|---|
| 20 | 10 | 214 | 0.00419 | 51.07 |
| 20 | 10 | 222 | 0.00884 | 25.11 |
| 20 | 10 | 227 | 0.00611 | 37.15 |
| 20 | 10 | 214 | 0.00473 | 45.24 |
| 40 | 30 | 1011 | 0.0169 | 59.82 |
| 40 | 40 | 1045 | 0.0158 | 66.14 |
| 40 | 27 | 979 | 0.0522 | 18.75 |
| 40 | 40 | 1075 | 0.0143 | 75.17 |

GAS PROCESSING UNIT

For use in conjunction with the gas targets for ^{11}C and ^{15}O production, a computer-controlled Gas Processing Unit (GPU) has been developed that can be configured 1) to provide contaminant-free ^{15}O O_2 , 2) to convert ^{11}C CO_2 to ^{11}C CO (for use in blood volume determinations or as a precursor in subsequent radiosyntheses), or 3) to convert ^{15}O O_2 to ^{15}O CO (blood volume), ^{15}O CO_2 (blood flow), or ^{15}O H_2O . These remote automated conversions that can be performed by the GPU are extensions of processes and systems that are adequately described in the literature.^{21,22} The unit is shown in Figure 5.

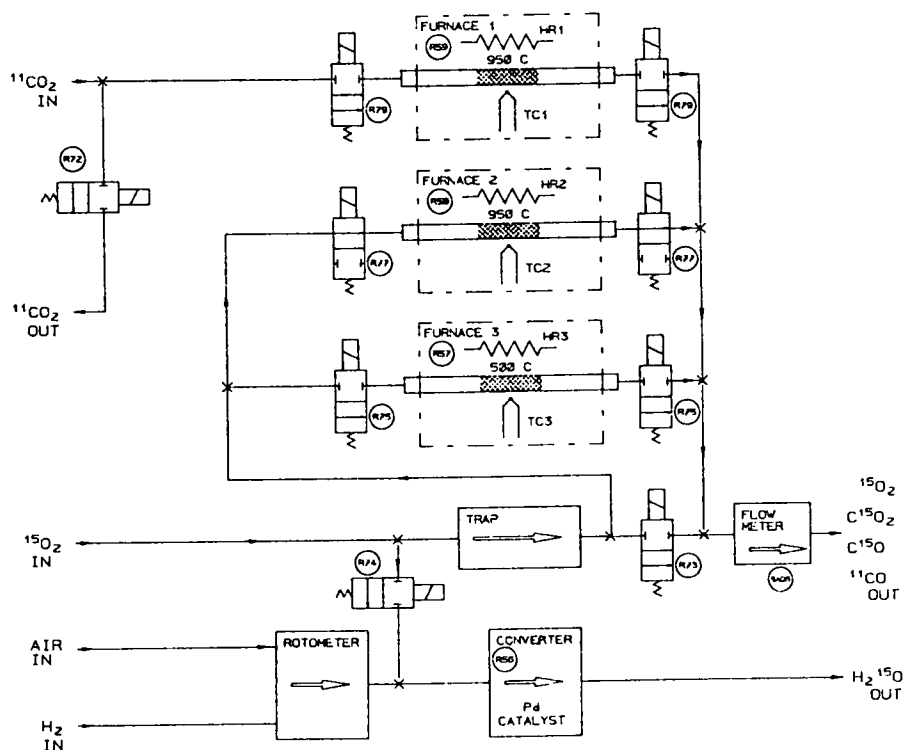


FIGURE 5. GAS PROCESSING UNIT

Features of the CTI Gas Processing Unit (GPU)

- 1) Unit performs computer-controlled conversions via a menu-driven selection format that provides the user access to the desired radiochemical;
- 2) Designed to minimize dead volume, and hence, decay loss of ^{15}O ;
- 3) Unit is equipped with appropriate materials for chemical conversion and purification that insures contaminant-free final products;
- 4) Unit is readily configured for either continuous or bolus delivery of radiolabeled gases;
- 5) Unlike production of some ^{15}O -labelled gases via deuterons, only one target gas mixture is required for production of these radiochemicals via the proton reaction.

^{11}C]HCN Unit

This single pass gas reaction system shown in Figure 6 (for use in subsequent synthesis of amino acids, CDG, etc.) has provisions for sampling ports to allow setups and analysis. The unit contains an integral control chassis which allows all parameters to be controlled and monitored by a PC-type computer through a STD bus.

A demonstration was performed using 10.4 MeV protons on nitrogen plus 1% oxygen for 40 min at $40\ \mu\text{A}$ (1950 mCi in the target at EOB). Sixty-five percent of this activity (200 to 70 psia target pressure decrease) was dispensed and passed through the system with a 75 mL/min Helium sweep. At the end of 14 min there were 697 mCi of ^{11}C]HCN trapped in the soda line. The decay-corrected conversion yield was 89%. The first hospital unit is being set up at the University of Tennessee.

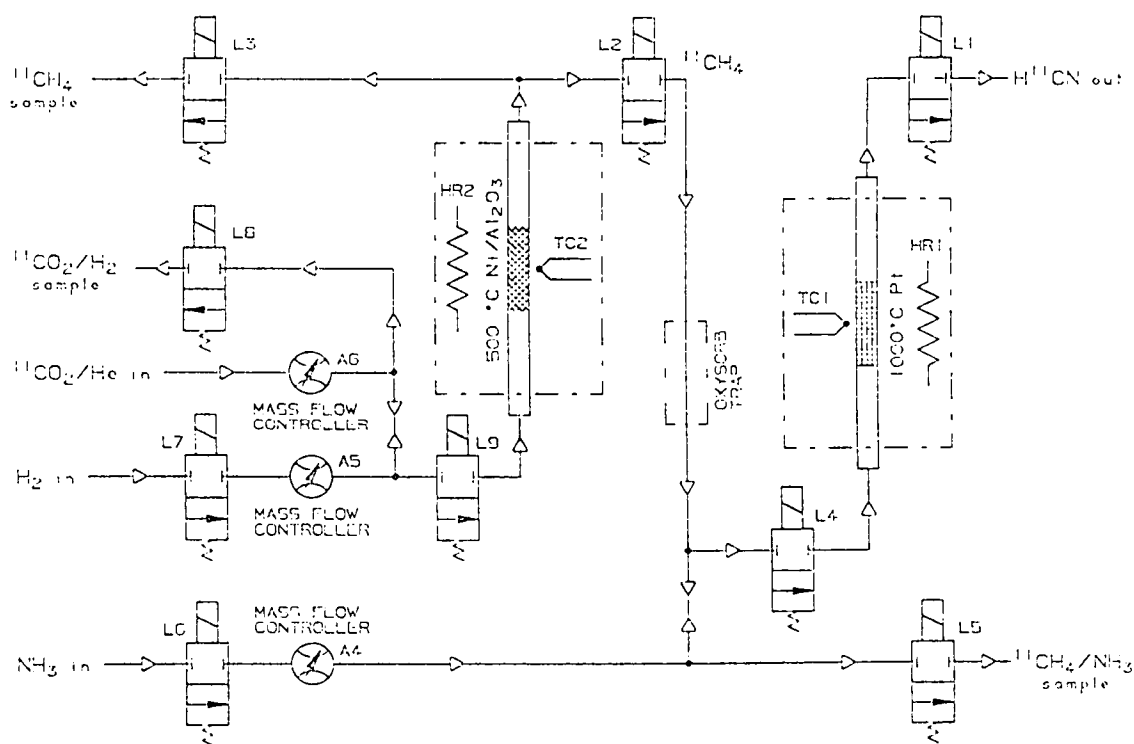


FIGURE 6. ^{11}C]HYDROGEN CYANIDE PRODUCTION

Gas Target Heat Transfer

We have observed from pressure vs. beam current measurements that our 11.9 cc gas targets exhibit two distinctly separate patterns as shown in Figure 7. One occurs below 10 μA beam current and exhibits a rapid increase in target pressure (temperature) with beam current. The other occurs at currents above 10 μA and exhibits a much less rapid but linear increase in pressure with increasing beam current. The abrupt change in the slope of the pressure vs. beam current curves occurs at the same current regardless of target loading or target gas (for both nitrogen and helium).

Heat transfer film coefficients between the target gas and the target wall have been calculated from the data gathered for a 225 psia nitrogen target load shown in Figure 8. The low current mode ($<10 \mu\text{A}$) results in a heat transfer coefficient of $125 \text{ W/m}^2 / ^\circ\text{C}$. The high current mode ($>10 \mu\text{A}$) for the same conditions results in a heat transfer coefficient of $273 \text{ W/m}^2 / ^\circ\text{C}$. The target was a 100 mm long truncated cone having an entrance of 10.0 mm diameter and an exit of 14.5 mm diameter. The data in Figures 7 and 8 show similar behavior at other target loadings.

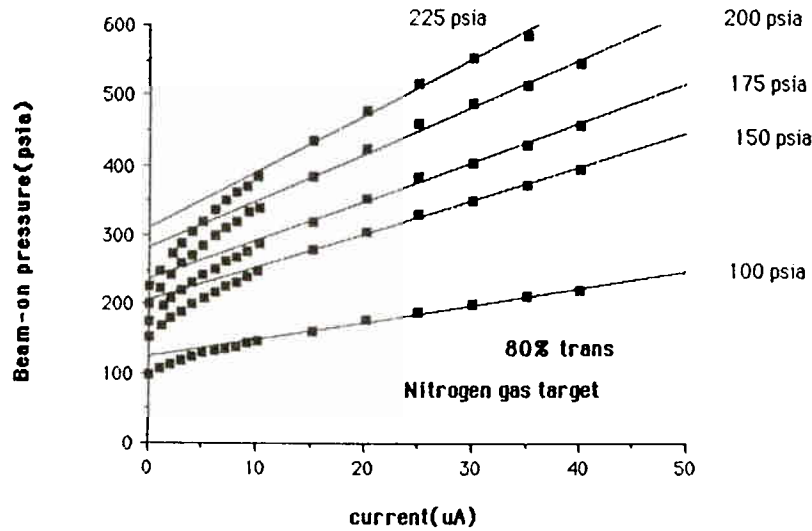


FIGURE 7. GAS TARGET PRESSURE RISE

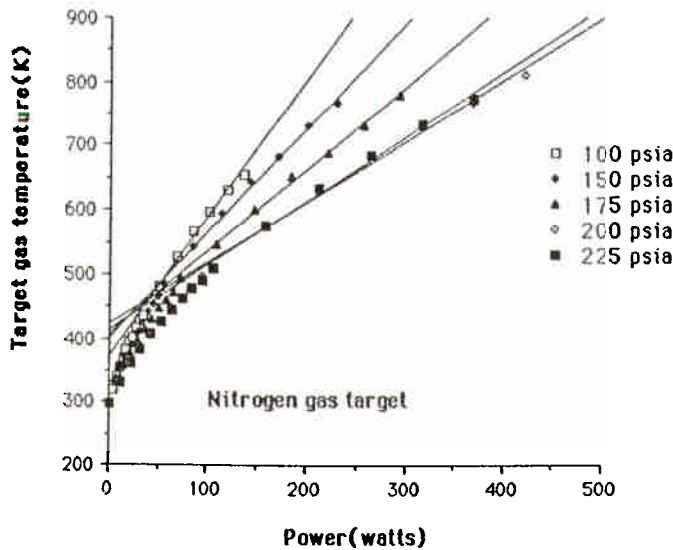


FIGURE 8. GAS TARGET TEMPERATURE

The discontinuity in heat transfer coefficient suggests two modes of heat transfer. Laminar flow with conductive heat transfer may be occurring at low current, while turbulent flow with convective heat transfer may be occurring at high current. Heselius' data shows essentially the same effect.¹⁶ These measurements show the discontinuity in cooling modes at approximately $2\ \mu\text{A}$ beam current. This might be expected since Heselius used a 56 cc target volume while our target volume was 11.9 cc. The Reynolds number, which governs the transition from laminar to turbulent flow, depends linearly on the system dimension and velocity. Thus targets with larger dimensions reach the critical Reynolds number at lower velocities.

We speculate that at low beam currents ($<10\ \mu\text{A}$) there is circulating laminar flow induced by momentum transfer from the beam. Under these conditions, conductive heat transfer predominates. Increasing the beam current increases the velocity of the flow until the critical Reynolds number is reached. Above this critical value, flow in the target is turbulent and convective heat transfer predominates.

If this is true, one might expect a relatively uniform density distribution in our zero-dead-volume target, without target thinning on the beam axis. Our observations support this hypothesis, showing little or no thinning even at $40\ \mu\text{A}$ beam currents.

CONCLUSION

The work reported here contributes to making PET available to a wider range of users than in the past, due to simplified isotope production and radiochemical synthesis. It is likely that further simplification and automation by a variety of researchers will play a critical role in the rapidly developing field of clinical PET. We predict an expansion of available target and synthesis systems, as well as the development by others of systems for automatically preparing and delivering patient doses using remote techniques instead of syringe manipulations performed by technicians.

ACKNOWLEDGEMENT

The authors would like to acknowledge the PET centers indicated by reference⁵ in the introduction section, for providing helpful data and analysis acquired during the use of CTI target and radiochemical systems in a clinical environment. Craig Harris has been particularly thorough in his assessment of the ^{18}F fluoride and ^{13}N ammonia target performance at Duke University, and we appreciate his collaborative input in characterizing and improving these systems.

We would also like to thank Tom Rathmann and Todd Cort of our Berkeley research group for assistance in the preparation of this paper.

REFERENCES

- 1) B.W. Wieland, G.O. Hendry and D.G. Schmidt, *J Label Compds Radiopharm.*, 23:1187-1189 (1986).
- 2) B.W. Wieland, G.O. Hendry, D.G. Schmidt, G.T. Bida, and T.J. Ruth, *J Label Compds Radiopharm.*, 23:1205-1207 (1986).
- 3) B.W. Wieland, D.G. Schmidt, G.T. Bida, T.J. Ruth, and G.O. Hendry, *J Label Compds Radiopharm.*, 23:1214-1216 (1986).
- 4) G.T. Bida, B.W. Wieland, T.J. Ruth, D.G. Schmidt, G.O. Hendry, and R.E. Keen, *J Label Compds Radiopharm.*, 23:1217-1218 (1986).
- 5) UCLA, U. of Wis. (Madison,WI), Duke U. (Durham,NC), U. of Tenn. (Knoxville, TN), Hospital San Raffaele (Milan, Italy).
- 6) U. of Tenn., Hospital San Raffaele.
- 7) Siemens RDS 112.
- 8) H.C. Padgett, D.G. Schmidt, A. Luxen, G.T. Bida, N. Satyamurthy, and J.R. Barrio, *Appl. Rad. Isot.*, 40:433-445 (1989).
- 9) Vanderbilt U. (Nashville, TN), Creighton U. (Omaha, NE).

- 10) CTI PET Systems, Inc., Knoxville, TN.
- 11) Siemens Medical Systems and Siemens Gammasonics, Inc., Hoffman Estates, IL.
- 12) G.T. Bida, N. Satyamurthy, B.W. Wieland, and T.J. Ruth, Proceedings of the 2nd Workshop on Targetry and Target Chemistry, Heidelberg, 1987, p.19.
- 13) R.J. Nickles, M.E. Daube, and T.J. Ruth, Int. J. Appl. Radiat. Isot., 35:117 (1984).
- 14) O. Solin, and J. Bergman, J Label Cmpds and Radiopharm., 23:1202 (1986).
- 15) J.J. Sunderland, O.T. de Jesus, C.C. Martin, and R.J. Nickles, J. Nucl. Med., 30 (Suppl.):972 (1989).
- 16) S.J. Heselius, P. Malmborg, O. Solin, and B. Langstrom, Appl. Radiat. Isot., 38:49-57 (1987).
- 17) G.T. Bida, T.J. Ruth and A.P. Wolf, Radiochim Acta., 27:181 (1980).
- 18) J.C. Clark, and S. Reiffers, Proceedings of the First Workshop on Targetry and Target Chemistry, Heidelberg, 1985, p.17.
- 19) R. Iwata, T. Ido, T. Takahashi, H. Nakanishi, and S. Iada, Appl. Radiat Isot., 38: 97-102 (1987).
- 20) M. Sajjad, R.M. Lambrecht, and A.P. Wolf, Radiochim. Acta., 36:159 (1984).
- 21) J.C. Clark, and P.D. Buckingham, Short-lived Radioactive Gases for Clinical Use, Butterworth and Co., London, 1975.
- 22) W. Vaalburg, and A.M.J. Paans, Chapter 2 in Radionuclides Production, Vol II, F. Helus, ed., CRC Press, Boca Raton, FL. 1983.